Discovery of novel diarylpyrimidines as potent HIV NNRTIs via a structure-guided core-refining approach

ARTICLE *in* EUROPEAN JOURNAL OF MEDICINAL CHEMISTRY · APRIL 2014

Impact Factor: 3.45 · DOI: 10.1016/j.ejmech.2014.04.036 · Source: PubMed

European Journal of Medicinal Chemistry 80 (2014) 112–121

Contents lists available at ScienceDirect

European Journal of Medicinal Chemistry

journal homepage: http://www.elsevier.com/locate/ejmech

Original article

Discovery of novel diarylpyrimidines as potent HIV NNRTIs via a structure-guided core-refining approach

Xiao Li [a], Wenmin Chen [a], Ye Tian [a], Huiqing Liu [b], Peng Zhan [a,*], Erik De Clercq [c], Christophe Pannecouque [c], Jan Balzarini [c], Xinyong Liu [a,*]

[a] Department of Medicinal Chemistry, Key Laboratory of Chemical Biology (Ministry of Education), School of Pharmaceutical Sciences, Shandong University, 44 West Culture Road, 250012 Jinan, Shandong, PR China
[b] Institute of Pharmacology, School of Medicine, Shandong University, 44 West Culture Road, 250012 Jinan, Shandong, PR China
[c] Rega Institute for Medical Research, KU Leuven, Minderbroedersstraat 10, B-3000 Leuven, Belgium

ARTICLE INFO

Article history:
Received 3 December 2013
Received in revised form
8 April 2014
Accepted 11 April 2014
Available online 13 April 2014

Keywords:
HIV-1
HIV-2
DAPY
Anti-HIV activities
Structure–activity relationships
Molecular modeling

ABSTRACT

Guided by crystal structures of HIV-1 RT/DAPY complex and molecular modeling studies, a series of novel DAPY derivatives were rationally designed, synthesized and evaluated for their anti-HIV activities. Among them, 16 compounds significantly inhibited HIV-1 IIIB replication with EC_{50} values lower than 66 nM. Particularly, compound 7a was the most potent inhibitor against HIV-1 wild-type and double RT mutant HIV-1 strain K103N/Y181C, with an EC_{50} value of 2.5 nM (SI = 13,740) and 0.33 μM (SI = 107), respectively. Unexpectedly, compound 8c was found to show moderate anti-HIV-2 potency (EC_{50} = 5.57 μM). Preliminary structure–activity relationships (SARs) and molecular modeling of these new analogues were also discussed in detail.

1. Introduction

Acquired immunodeficiency syndrome (AIDS) mainly caused by human immunodeficiency virus type-1 (HIV-1), remains a worldwide health threat, with approximately 34 million people living currently with HIV and more than 25 million deaths since it was first identified [1]. Despite the dramatically decreased in morbidity and mortality from HIV-1 infection by introducing the highly active antiretroviral therapy (HAART), a definitive cure of AIDS by chemotherapeutics still has a long way to go [2,3].

HIV-1 non-nucleoside reverse transcriptase (RT) inhibitors (NNRTIs) with unique antiviral potency, high specificity and low cytotoxicity have played an indispensable role in HAART [4,5]. The development of novel chemical entities with high inhibition for the mutated strains has always been a very active research field in the past two decades [6–9]. Especially, considerable efforts have been devoted to the structural modification of diarylpyrimidines (DAPYs), a family of NNRTIs with remarkable anti-HIV-1 activity, leading to the discovery of two approved drugs, etravirine (TMC125, **1**) and rilpivirine (TMC278, **2**) (Fig. 1) and other highly potent compounds against both HIV-1 wild-type and mutant strains, which provide additional options for HAART regimen [10,11].

Currently, with attempts to increase the inhibitory efficacy against HIV-1 and to further explore the structural features required for anti-HIV-1 activity, different types of modifications have been carried out in the DAPY scaffold, including the left wing (L) that linked to the 4-position of the pyrimidine core, the right wing (R), the central pyrimidine ring (C), and the linker [12–14]. Moreover, the disclosed crystal structures of the HIV-1 RT/DAPY complex and/or molecular modeling studies have pointed out that the presence of three key chemical features was closely related to the RT inhibition, i.e., the left aryl wing, extending into the NNRTI binding pocket (NNIBP) to form an important hydrophobic interaction, and a para-substituted aniline moiety in the right wing, interacting with an aminoacid residue by a dipole–dipole

Abbreviations: AIDS, acquired immunodeficiency syndrome; HIV-1, human immunodeficiency virus type-1; HAART, highly active antiretroviral therapy; NNRTIs, non-nucleoside reverse transcriptase inhibitors; DAPYs, diarylpyrimidines; SARs, structure–activity relationships; NNIBP, NNRTI binding pocket.

* Corresponding authors.
E-mail addresses: zhanpeng1982@sdu.edu.cn (P. Zhan), xinyongl@sdu.edu.cn (X. Liu).

http://dx.doi.org/10.1016/j.ejmech.2014.04.036
0223-5234/

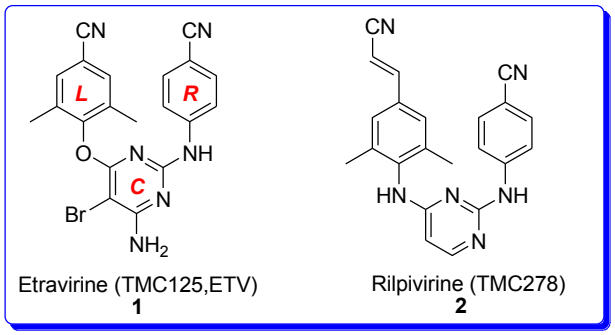

Fig. 1. The structures of two DAPY NNRTIs drugs. For convenience, we refer to the structural components of DAPYs as the left wing (L), the right wing (R), the central pyrimidine ring (C), bridge L–C (O or NH linker), and bridge C–R (NH linker).

interaction, as well as the NH linker, forming a key hydrogen bond with the backbone of K101, which are crucial for the drug resistance profile (Fig. 2) [15,16]. Initial molecular modeling suggested that the substitution at the position of the N_1 pyrimidine could potentially provide a vector to access consecutive lysine residues (Lys101–Lys104) in the NNIBP (Fig. 2), and the overall conformation of the inhibitor should be largely preserved.

Supported by these findings and with the aim to further explore untapped chemical space in NNIBP and obtaining more potent back-up series of DAPY derivatives, in this study, we designed and synthesized new DAPY analogues in which the positions of nitrogen atoms in the central pyrimidine ring were changed, and nitro, amino and other nitrogen-containing groups were introduced at the primary position, supposing that the additional hydrogen bonds with surrounding residues could be formed by extended different types of nitrogen. Meanwhile, the two phenyl rings in the left and right wings and the NH linker were maintained in view of their paramount importance in parent drugs (Fig. 3). Thus, this study will highlight the synthesis, biological evaluation of novel DAPY derivatives, and also, SARs will be discussed according to the antiviral activity and molecular docking results.

2. Results and discussion

2.1. Chemistry

To achieve the synthesis of the target compounds 6–9, the steps outlined in Scheme 1 were adopted. Briefly, intermediate 5 was synthesized from two commercially available materials, 2,4-dichloro-5-nitropyrimidine (3) and 4-aminobenzonitrile (4), by a nucleophilic substitution reaction [17,18]. Treatment of 5 with the different substituted phenols and potassium carbonate under at 60 °C in DMF gave the target compounds 5-nitro-pyrimidine series 6a–g [19,20]. The nitro group on the central ring was treated with a mild reductant, stannous chloride (6c, 6d, 6e, 6f) or with hydrogenation catalyzed by Pd/C (5–10%) in anhydrous ethanol (6a, 6b, 6g) to afford the 5-amino-pyrimidine series 7a–g, which were then converted into the trifluoroacetamide series 8a–g and acetamide 9a–g, by acylation reaction with trifluoroacetic anhydride and acetylchloride, respectively [21,22]. The newly synthesized compounds were characterized by physicochemical and spectral means, and both analytical and spectral data of all the compounds were found in full agreement with the proposed structures.

2.2. Biological activity

The newly prepared DAPY derivatives (compounds 6–9) were evaluated for their anti-HIV activity in MT-4 cell cultures infected

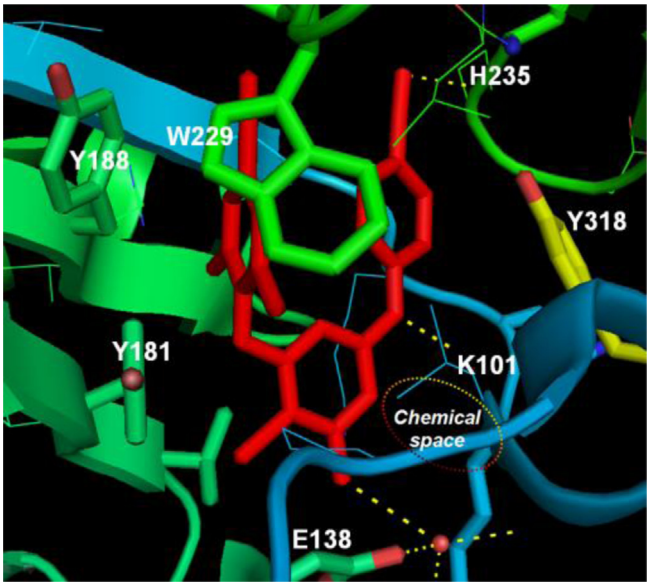

Fig. 2. Mode of TMC125 (red) at the NNIBP of wt RT (PDB code: 3MEC). Ligand is shown in red. Hydrogen bonds are depicted as yellow dashes. The figure was generated using PyMol (www.pymol.org). The design of new DAPY derivatives was guided by a model of interaction between the lead compound TMC125 and the NNIBP. (For interpretation of the references to color in this figure legend, the reader is referred to the web version of this article.)

with wild-type HIV-1 strain (III_B), double mutant HIV-1 strain RES056 (K103N + Y181C), and HIV-2 strain (ROD), respectively, in parallel with their cytotoxicities. FDA-approved nevirapine (NVP) and delavidine (DLV) were used as reference drugs for comparison. The biological results are represented as EC_{50} values (anti-HIV activity), CC_{50} values (cytotoxicity) and SI values (selectivity index, given by the CC_{50}/EC_{50} ratio).

As shown in Table 1, the biological results clearly indicated that most derivatives proved to be highly effective in inhibiting HIV-1 IIIB replication at double-digit nanomolar ranges. Notably, compounds **7a**, **7b** were the most potent inhibitors against HIV-1 IIIB replication with an EC_{50} value of 2.5 nM and 7.2 nM, respectively, which were superior to those of the reference drugs NVP, DLV, EFV, AZT and 3 TC. Besides, some other compounds including **6a**, **6b**, **6e**, **7c**, **7d**, **7e**, **7f**, **7g**, **8a**, **8**b, **8c**, **8d** and **8e**, also exhibited favorable potency against the HIV-1 IIIB strain with EC_{50} values in the range of 23–66 nM, which were more potent than that of NVP, DLV and 3TC.

Besides the excellent activity against the HIV-1 wild-type strain, **7a** was also the most active compound against HIV-1 double-mutant strain K103N/Y181C (RES056) with EC_{50} value of 0.33 μM and SI of 107. The potency of **7a** against mutant HIV-1 in this assay was higher than that of NVP, DLV, and 3TC, and similar to that of EFV. In addition, it is interesting to note that, except for 2,6-disubstituted phenoxyl derivatives (**7f**, **8f**), other compounds with R^2 substituted with NH_2 or $NHCOCF_3$ (**7a**, **8a**, **7b**, **8b**, **7c**, **8c**, **7d**, **8d**, **7e**, **8e**, **7g**, **8g**) displayed remarkable activities against HIV-1 RES056 strain with EC_{50} values in micromolar concentration ranges.

As can be seen in Table 1, the anti-HIV activity (IIIB and RES056 strains) is dramatically depended on the nature of the substituents at C-5 of the pyrimidine ring. Significant difference in antiviral activity against HIV-1 IIIB and RES056 strains can be observed, with the general order: 7a–g series ($R^2 = NH_2$) > 8a–g series ($R^2 = NHCOCF_3$) > 6a–g series ($R^2 = NO_2$) >> 9a–g series ($R^2 = NHCOCH_3$), indicating amino group as hydrogen bond donor was the preferred substituent compared with hydrogen bond acceptor group nitro, while introduction of $NHCOCH_3$ severely

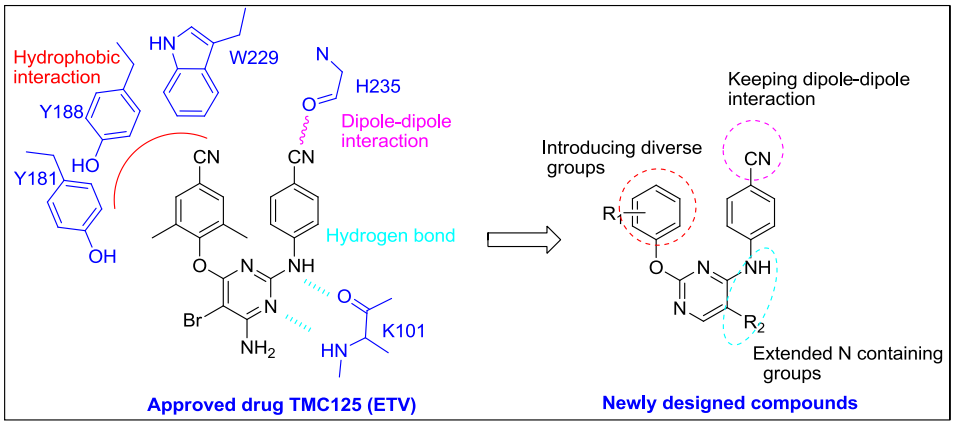

Fig. 3. Schematic diagram of the binding mode of TMC125 with NNIBP and design of novel DAPY derivatives via a structure-guided core-refining approach.

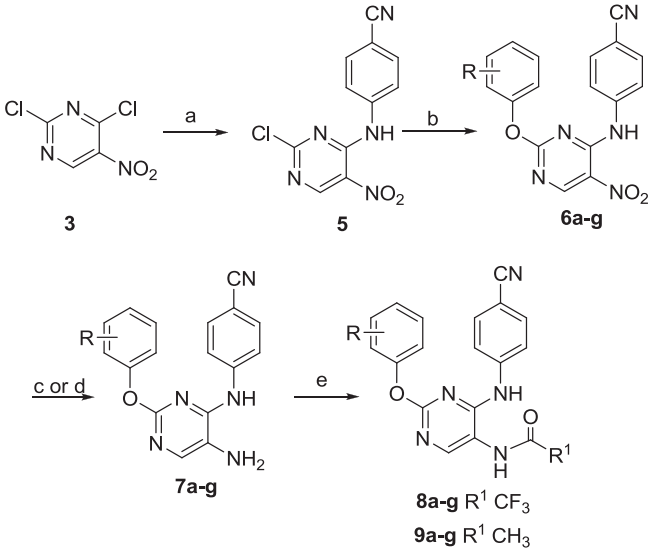

Scheme 1. The synthetic route of target compounds. Reagents and conditions: (a) 4-aminobenzonitrile (4), THF, Et_3N, 0 °C. (b) DMF, K_2CO_3, 60 °C. (c) $SnCl_2 \cdot 2H_2O$, EtOH. (d) EtOH, Pd/C, rt. (e) THF, CH_2Cl_2, Et_3N, $CF_3COOCOCF_3$ or CH_3COCl.

impaired the activity, which might reflect a spatial restriction in the target site of the HIV RT. Besides, it was clearly revealed that although trifluoroacetylation of NH_2 group (8a–g) makes anti-HIV activity (IIIB and RES056) reduced to a certain extent, while still keep on the same active order of magnitudes as amino derivatives(7a–g), which is in sharp contrast to other two series(6a–g, 9a–g).

In comparison with the substituent effect at the C_2-position of the pyrimidine ring, SAR analysis of the left ring moiety was summarized as the following: 2,6-Me-4-CN-phenoxy substitution was found to be the best functional group conferring high potency against HIV-1 IIIB and RES056 strains. With regard to the activity against the HIV-1 IIIB strain, substitution at 4-position of the 2,6-Me-phenoxy dominated the antiviral potency and a declining trend was found (7a–g series, 8a–g series, and 9a–g series) with the following different groups at the 4-position: 4-CN > 4-Me > 4-Br > 4-CHO. Compounds in the 6a–g series have a slightly different in the activity sequence: 4-Me > 4-CN > 4-Br > 4-CHO. Among the four series of compounds, only compounds in 7a–g series gave a parallel order of activity against HIV-1 IIIB and RES056 strains (4-CN > 4-Me > 4-Br > 4-CHO).

Regarding the potency against double-mutant strain RES056, only the 7a–g series and 8a–g series exhibited the antiviral activities. The active sequence of the substitutions at the C_2 position of the pyrimidine core was as follows: 2,6-Me-4-CN > 2,4,6-Me > 2,6-Me-4-CHO > 2,6-Cl-4-H. Analogues with the 2,6-Cl-4-H-phenoxy substituent were found to be the worst inhibitors against the RES056 strain. Therefore, it is further confirmed that the nature of the substituents with a suitable volume and high hydrophobicity in the left wing is crucial for these novel DAPY analogues to have improved drug resistance profiles.

To the best of our knowledge, most NNRTIs are specific for HIV-1 and only a few might exert some minimal inhibition against HIV-2. Unexpectedly, two trifluoroacylating compounds **8c** and **8e** have moderate activity against HIV-2, in particular, **8c** presented with an EC_{50} value of 5.57 μM, suggesting that a potential interaction may exist between these inhibitors and HIV-2 RT or other targets.

2.3. Inhibition of HIV-1 RT

With the aim to further confirm the drug target or other targets, two most active compounds **7a**, **7b** were selected to be evaluated in an enzymatic assay against highly purified recombinant HIV-1 RT using hybrid poly (A) · oligo $(dT)_{15}$ (9 $A_{260\ nm}$/ml), lyophilizate as template primer. As shown in Table 2, compounds **7a**, **7b** exhibited high inhibition of enzymatic activity with an IC_{50} value of 2.1 μM, 5.2 μM, respectively, which were more active than that of TMC125 (ETV, IC_{50} = 6.5 μM).

2.4. Molecular modeling analysis

To shed light on the preferred interaction mode in the NNIBP and rationalize SARs of these derivatives, a molecular docking study of the most active compound **7a** was performed using software SYBYL-X. The theoretical binding mode to the NNIBP is shown in Fig. 4.

As expected, compound **7a** had nearly the same binding mode in wt HIV-1 RT as etravirine (ETV). Detailed analysis of the docking results revealed the following notable features: (1) the left wing of compound **7a** fitted into the important hydrophobic sub-pocket comprised of aromatic residues Y181, Y188, F227 and W229, exhibiting π–π interaction with these residues, while cyano group at para-position pointed to conservative amino acid W229 to form a dipole–dipole interaction. (2) Two hydrogen bonds were formed with backbone carbonyl and backbone amino of residue K101, improving the stability of RT-inhibitor complex and the affinity between RT and inhibitor. (3) The right aniline ring extended to the

Table 1
Activity against HIV-1 and cytotoxicity in MT-4 cells.

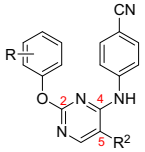

Compds	R	R^2	HIV-1IIIB		RES056		ROD		CC_{50} (μ)[b]
			EC_{50} (μ)[a]	SI[c]	EC_{50} (μM)	SI	EC_{50} (μM)	SI	
6a	2,6-Me, 4-CN	NO_2	0.062 ± 0.008	>4473	≥10.3.	><27	>274	><1	≥274
7a	2,6-Me, 4-CN	NH_2	0.002 ± 0.001	13740	0.33 ± 0.00	107	>35.1	<1	35.1 ± 4
8a	2,6-Me, 4-CN	$NHCOCF_3$	0.037 ± 0.007	>7470	5.0 ± 0.8	>55	>276	><1	>276
9a	2,6-Me, 4-CN	$NHCOCH_3$	1.8 ± 0.7	>169	>313	><1	>313	><1	>313
6b	2,4,6-Me	NO_2	0.042 ± 0.010	≥5480	>252	><1	>252	><1	≥252
7b	2,4,6-Me	NH_2	0.007 ± 0.005	1432	0.75 ± 0.17	14	>10	<1	10 ± 9.8
8b	2,4,6-Me	$NHCOCF_3$	0.039 ± 0.004	6254	32 ± 9	8	>242	<1	242 ± 14
9b	2,4,6-Me	$NHCOCH_3$	9.3 ± 6.7	>35	>322	><1	>322	><1	>322
6c	2,4,6-Cl	NO_2	7.4 ± 1.0	≥3	>25.	><1	>25	><1	≥25
7c	2,4,6-Cl	NH_2	0.012 ± 0.001	2311	2.8 ± 1.8	9	>26	<1	26 ± 3
8c	2,4,6-Cl	$NHCOCF_3$	0.064 ± 0.034	>6968	24 ± 12	>11	5 ± 1	>45	>248
9c	2,4,6-Cl	$NHCOCH_3$	1.9 ± 0.6	17	>33	<1	>33	<1	33 ± 1
6d	2,4,6-Br	NO_2	3.9 ± 0.3	5	>20	<1	>20	<1	20 ± 2
7d	2,4,6-Br	NH_2	0.050 ± 0.017	750	4.9 ± 0.6	8	>37	<1	37 ± 25
8d	2,4,6-Br	$NHCOCF_3$	0.035 ± 0.002	484	2.9 ± 0.4	6	>17.0	<1	17.0 ± 1
9d	2,4,6-Br	$NHCOCH_3$	20 ± 1.2	6	>118	<1	>118	<1	118 ± 8
6e	2,6-Me, 4-Br	NO_2	0.063 ± 0.025	≥3199	>202.3	><1	>202.3	><1	≥202
7e	2,6-Me, 4-Br	NH_2	0.046 ± 0.002	702	4.8 ± 1.7	6	>31	<1	31 ± 3
8e	2,6-Me, 4-Br	$NHCOCF_3$	0.053 ± 0.012	>4647	11 ± 7	>23	36 ± 2	>7	>246
9e	2,6-Me, 4-Br	$NHCOCH_3$	32 ± 5	5	>147	<1	>147	<1	147 ± 8
6f	2,6-Cl	NO_2	3.2 ± 0.3	≥65	>206	><1	>206	><1	≥206
7f	2,6-Cl	NH_2	0.023 ± 0.001	1410	>33	<1	>33	<1	33 ± 3
8f	2,6-Cl	$NHCOCF_3$	0.14 ± 0.01	1355	>190	<1	>190	<1	190 ± 46
9f	2,6-Cl	$NHCOCH_3$	32 ± 4.4	6	>193	<1	>193	<1	193 ± 15
6g	2,6-Me, 4-CHO	NO_2	0.61 ± 0.31	59	>37	<1	>37	<1	37 ± 2
7g	2,6-Me, 4-CHO	NH_2	0.066 ± 0.00	≥551	8.4 ± 0.5	≥4	>34	><1	≥34
8g	2,6-Me, 4-CHO	$NHCOCF_3$	0.48 ± 0.28	≥441	35 ± 15	≥6	>216	><1	≥216
9g	2,6-Me, 4-CHO	$NHCOCH_3$	29 ± 2	8	>236	<1	>236	<1	236 ± 15
NVP			0.22 ± 0.06	>67	4.0 ± 3.7	>4	>15	><1	>15
3TC			3.7 ± 2.2	>23	21 ± 9	>4	>87	><1	>87
AZT			0.007 ± 0.003	>12235	0.015 ± 0.010	>5959	0.011 ± 0.01	>7716	>93
EFV			0.006 ± 0.000	>1133	0.31 ± 0.22	>21	>6.3	><1	>6.3
DLV			0.507 ± 0.506	>72	>36	><1	>36	><1	>36
ETV[d]			0.002 ± 0.0004	12884	0.034 ± 0.005	1817	>27	<1	27 ± 11

[a] EC_{50}: concentration of compound required to achieve 50% protection of MT-4 cell cultures against HIV-1-induced cytotoxicity, as determined by the MTT method.
[b] CC_{50}: concentration required to reduce the viability of mock-infected cell cultures by 50%, as determined by the MTT method.
[c] SI: selectivity index, the ratio of CC_{50}/EC_{50}.
[d] ETV: etravirine. The data were obtained from the same laboratory (Rega Institute for Medical Research, KU Leuven, Belgium).

Table 2
RT Inhibitory activity of compounds 7a and 7b.

Compd.	7a	7b	TMC125
IC_{50} (μM)[a]	2.1	5.2	6.5

[a] IC_{50}: Inhibitory concentration of tested compounds required to inhibit biotin deoxyuridine triphosphate (biotin-dUTP) incorporation into the HIV-1 RT by 50%.

surface of solvent and protein, and the para-substituted CN interacted with amino acid residue H235. Overall, all of these molecular interaction analyses were in accordance with the biological results. Obviously, the novel compounds showed excellent activity against wt HIV-1 because of specific interactions with key amino acid residues in NNIBP (Fig. 4a).

In addition, the moderate potency of **7a** against K103N/Y181C double mutant HIV-1 was rationally explained by molecular modeling results as well. As shown in Fig. 4b, two crucial hydrogen bonds between C_5—NH_2, NH linker and peptidic carbonyl oxygen of K101 were maintained. Even more surprising, a potential hydrogen bond was formed with easily mutated amino acid N103, providing additional affinity with mutant HIV-1 RT. However, **7a** still displayed less potent activity against K103N/Y181C resistant mutant RT strains, which might be due to the mutation at the Y181 side chain that led to partial loss of the dependent π—π interaction and finally resulted in decreased anti-HIV activity.

Based on the above analysis of molecular modeling, further optimization strategy can be concluded that (1) keeping hydrogen bonds with the backbone of residue K101 as well as mutant amino acid such as N103 is indispensable for obtaining improved activity against both HIV-1 IIIB and RES056 strains. (2) a hydrophobic flexible substituent on the left wing of DAPY might insert into the narrow tunnel on the NNRTI binding site and interact with the conserved W229 to enhance antiviral potency against resistant viral strains.

3. Conclusion

In summary, through structure-guided rescaffolding (core refining) and side-chain optimization of the approved drug

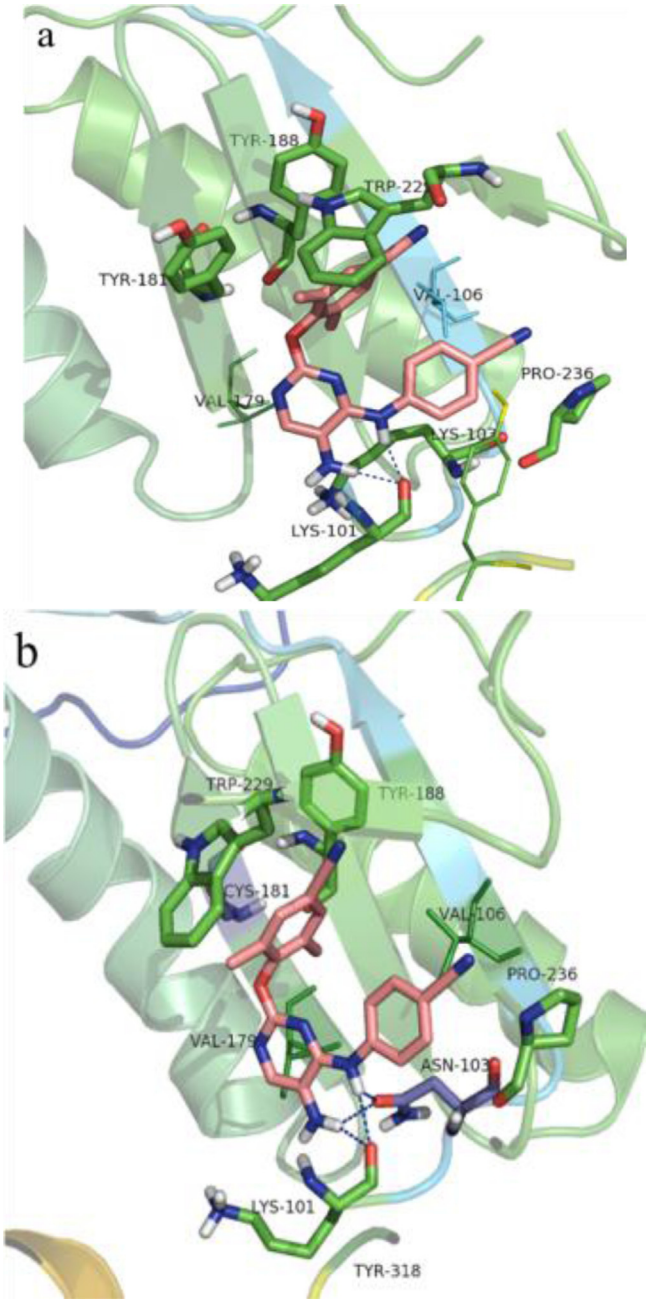

Fig. 4. Predicted binding modes between the new compounds 7a and NNIBP of (a) wt HIV-1 RT (PDB code: 3MEC) and (b) K103N/Y181C double mutant RT structure (PDB code 3BGR).

TMC125, a series of novel DAPY derivatives were designed, synthesized and evaluated for their antiviral activity against wt HIV-1, a double-mutated HIV-1 strain (K103N/Y181C) and HIV-2 (ROD) in MT-4 cells, as well as against HIV-1 RT activity of some selected compounds. It was demonstrated that most compounds showed excellent activity against wt HIV-1 with EC_{50} values in the low nanomolar concentration range (7a, $EC_{50} = 2.5$ nM, SI = 13740; 7b, $EC_{50} = 7.2$ nM, SI = 1432) and moderate activity against resistant mutant strain K103N/Y181C of HIV-1 with EC_{50} values in the submicromolar concentration range (7a, $EC_{50} = 0.33$ μM, SI = 107). A brief discussion of the SARs expatiated that the nature of the substituent on left ring of the central pyrimidine ring had a significant impact on the antiviral activity. In addition, molecular docking results were used to rationalize these biological data, which will be beneficial to further design more potent anti-HIV-1 agents.

4. Experimental section

4.1. Chemistry

4.1.1. Synthetic procedures and analytical datas for all new compounds

Mass spectrometry was performed on an API 4000 triple-quadrupole mass spectrometer (Applied Biosystems/MDS Sciex, Concord, ON, Canada). ^{1}H NMR and ^{13}C NMR spectra were recorded on a Bruker AV-400 spectrometer (Bruker BioSpin, Switzerland), using solvents as indicated ($CDCl_3$ or DMSO-d_6). Chemical shifts were reported in δ values (ppm) with tetramethylsilane as the internal reference, and J values were reported in hertz (Hz). Melting points (mp) were determined on a micromelting point apparatus (Tian Jin Analytical Instrument Factory, Nankai, Tianjin, China). Flash column chromatography was performed on columns packed with silica gel 60 (200–300 mesh) (Qingdao waves silica gel desiccant co., Ltd, Qingdao, China). Thin layer chromatography was performed on pre-coated HUANGHAI® HSGF254, 0.15–0.2 mm TLC-plates (Yantai Jiangyou Silica Gel Development Co., Ltd., Yantai, Shandong, China).

4.1.2. General procedure for the synthesis of 4-(2-chloro-5-nitropyrimidin-4-ylamino)benzonitrile (5)

To a solution of 2,4-dichloro-5-nitropyrimidine 3 (0.39 g, 2 mmol) in THF (15 mL) at 0 °C was slowly added THF solution of 4-aminobenzonitrile 4 (0.24 g, 2 mmol) and triethylamine (0.22 g, 2.2 mmol). The resulting mixture was stirred at 0 °C for 3 h (monitored by TLC). The solvent was removed under reduced pressure and water (20 mL) was added and extracted with CH_2Cl_2 (3 × 10 mL). Combined organic phase was washed with brine, dried over anhydrous Na_2SO_4, filtered and concentrated. Purification on silica gel (EA:PE = 1:8) gave 5 as a yellow solid.

4.1.3. General procedure for the synthesis of target compounds (6a–g)

Crude intermediate 5 was dissolved in anhydrous DMF (10 mL) in the presence of anhydrous K_2CO_3 (2 equiv) at room temperature followed by addition of appropriate substituted phenols (1.2 equiv). The reaction mixture was stirred at 60 °C for 5 h (monitored by TLC). The solvent was removed under reduced pressure, and water (20 mL) was added. Extracted with EA (3 × 10 mL), and the organic phase was washed with saturated sodium chloride (2 × 10 mL), and dried over anhydrous Na_2SO_4 to give the corresponding crude products, which were purified by flash column chromatography using ethyl acetate-petroleum ether system to afford the target compounds 6a–g, respectively.

4.1.4. General procedure for the synthesis of target compounds (7a–g)

Method A: The reaction system containing relevant compounds 6a, 6b, 6g (1 equiv), Pd/C (0.1 equiv) and 50 mL anhydrous EtOH was vacuumed and filled with excess hydrogen gas. The reaction mixture was kept for 10 h and then filtered out Pd/C, the solvent was evaporated under reduced pressure. The obtained crude product was washed by PE to give purified compound 7a, 7b, 7g. Method B: Compounds 6c, 6d, 6e, 6f obtained from last step (1 equiv) was dissolved in anhydrous EtOH (10 mL) in the presence of the reducing reagent stannous chloride (5 equiv). This reaction mixture was stirred at room temperature for 10 h (monitored by TLC). The solvent was removed under reduced pressure, and water (20 mL) was added. Extracted with EA (3 × 10 mL), and the organic

phase was washed with saturated sodium chloride (2 × 10 mL), and dried over anhydrous Na_2SO_4 to give the corresponding crude products, which were purified by flash column chromatography using methyl alcohol–dichloromethane system to afford the target compounds 7c, 7d, 7e, 7f, respectively.

4.1.5. General procedure for the synthesis of target compounds (8a–g)

Trifluoroacetic anhydride (1.2 equiv) was added dropwise under stirring to a solution of 7a–g (1.0 equiv) and triethylamine (2.0 equiv) in THF (20 mL) at 0 °C and stirred for 5 h (monitored by TLC). The solvent was removed under reduced pressure and water (20 mL) was added, then extracted with EA (3 × 10 mL). Combined organic phase was washed with brine, dried over anhydrous Na_2SO_4, filtered and concentrated. Purification on silica gel by using methyl alcohol–dichloromethane system gave target compounds 8a–g.

4.1.6. General procedure for the synthesis of target compounds (9a–g)

The procedure for the synthesis of target compounds (9a–g) is similar to 8a–g, except replacing trifluoroacetic anhydride with acetylchloride.

4.1.7. 4-(2-(4-Cyano-2,6-dimethylphenoxy)-5-nitropyrimidin-4-ylamino)benzonitrile (6a)

Yellow crystals, yield: 62.2%. mp: 227–230 °C. ^{1}H NMR (400 MHz, DMSO-d_6, ppm) δ: 10.50 (s, 1H, NH), 9.31 (s, 1H, C_6-pyrimidine-H), 7.53 (m, 6H, Ph-H, Ph′-H), 2.19 (s, 6H, 2 × CH_3). ^{13}C NMR (100 MHz, DMSO-d_6, ppm) δ: 164.69 (C_2-pyrimidine), 160.27 (C_4-pyrimidine), 154.60 (C_1-Ph′-N), 153.09 (C_6-pyrimidine), 140.08 (C_1-Ph-O), 133.13 (2 × C), 132.75 (2 × C), 132.35 (2 × C), 124.99, 121.61 (2 × CN), 118.11 (2 × C), 110.33, 109.00, 16.31 (2 × CH_3). ESI-MS: m/z 387.4 (M+1), 404.5 (M+18), $C_{20}H_{14}N_6O_3$ [386.11].

4.1.8. 4-(5-Amino-2-(4-cyano-2,6-dimethylphenoxy)pyrimidin-4-ylamino)benzonitrile (7a)

White powder, yield: 70.4%. mp: 218–221 °C. ^{1}H NMR (400 MHz, DMSO-d_6, ppm) δ: 8.93 (s, 1H, NH), 7.72 (s, 3H, C_6-pyrimidine-H, Ph-H), 7.63 (d, 2H, J = 8.80 Hz, 2H, Ph′-H), 7.56 (d, 2H, J = 8.80 Hz, 2H, Ph′-H), 4.93 (s, 2H, NH_2), 2.08 (s, 6H, 2 × CH_3). ^{13}C NMR (100 MHz, DMSO-d_6, ppm) δ: 155.66 (C_2-pyrimidine), 154.96 (C_4-pyrimidine), 150.36 (C_1-Ph′-N), 144.51 (C_6-pyrimidine), 141.55 (C_1-Ph-O), 133.30 (2 × C), 133.09 (2 × C), 132.95 (2 × C), 125.71, 119.72, 119.58 (2 × CN), 119.24, 107.99, 103.77, 16.28 (2 × CH_3). ESI-MS: m/z 357.4 (M+1), 474.4 (M+18) $C_{20}H_{16}N_6O$ [356.14].

4.1.9. N-(2-(4-Cyano-2,6-dimethylphenoxy)-4-(4-cyanophenylamino)pyrimidin-5-yl)-2,2,2-trifluoroacetamide (8a)

White powder, yield: 56.5%. mp: 255–257 °C. ^{1}H NMR (400 MHz, DMSO-d_6, ppm) δ: 9.25 (s, 1H, C_6-pyrimidine-H), 8.18 (d, J = 8.44 Hz, 2H, Ph′-H), 7.94 (d, J = 8.44 Hz, 2H, Ph′-H), 7.67 (s, 2H, Ph-H), 2.13 (s, 6H, 2 × CH_3). ^{13}C NMR (100 MHz, DMSO-d_6, ppm) δ: 161.82 (C_2-pyrimidine), 155.38 (C_4-pyrimidine), 153.50 (C_1-Ph-O), 153.37 (C_6-pyrimidine), 142.33 (C_1-Ph′-N), 141.94, 135.64, 133.84 (2 × C), 132.71 (2 × C), 132.43 (2 × C), 128.73, 128.31 (2 × CN), 118.53, 117.26, 114.88, 109.83, 16.41 (2 × CH_3). ESI-MS: m/z 435.5 ($C_{22}H_{17}F_2N_6O_2^+$), 452.4 (M+18), $C_{22}H_{15}F_3N_6O_2$ [452.12].

4.1.10. N-(2-(4-Cyano-2,6-dimethylphenoxy)-4-(4-cyanophenylamino)pyrimidin-5-yl) acetamide (9a)

White powder, yield: 54.2%. mp: 278–281 °C. ^{1}H NMR (400 MHz, DMSO-d_6, ppm) δ: 9.42 (s, 1H, NH), 9.22 (s, 1H, C_6-pyrimidine-H), 8.17 (s, 1H, NH), 7.74 (s, 2H, Ph-H), 7.64 (s, 4H, Ph′-H), 2.10 (s, 6H, 2 × CH_3), 2.09 (s, 3H, CH_3). ^{13}C NMR (100 MHz, DMSO-d_6, ppm) δ: 170.26 (C=O), 160.65 (C_2-pyrimidine), 156.80 (C_4-pyrimidine), 156.80 (C_1-Ph-O), 155.83 (C_6-pyrimidine), 154.31 (C_1-Ph′-N), 143.59, 133.08 (3 × C), 133.01 (2 × C), 120.67 (2 × C), 119.50 (2 × CN), 119.09, 115.07, 108.53, 104.83, 23.84, 16.21 (2 × CH_3). ESI-MS: m/z 399.3 (M+1), 416.5 (M+18), $C_{22}H_{18}N_6O_2$ [398.15].

4.1.11. 4-(2-(Mesityloxy)-5-nitropyrimidin-4-ylamino)benzonitrile (6b)

Yellow crystals, yield: 65.8%. mp: 186–189 °C. ^{1}H NMR (400 MHz, DMSO-d_6, ppm) δ: 10.44 (s, 1H, NH), 9.34 (s, 1H, C_6-pyrimidine-H), 7.43 (s, 4H, Ph′-H), 6.99 (s, 2H, Ph-H), 2.40 (s, 3H, CH_3), 2.07 (s, 6H, 2 × CH_3). ^{13}C NMR (100 MHz, DMSO-d_6, ppm) δ: 165.70 (C_2-pyrimidine), 160.41 (C_4-pyrimidine), 154.37 (C_6-pyrimidine), 147.91 (C_1-Ph′-N), 140.52 (C_1-Ph-O), 135.83, 132.99 (2 × C), 129.69 (2 × C), 129.56 (2 × C), 124.39, 121.77, 121.37, 118.47, 108.21, 20.89 (CH_3), 16.24 (2 × CH_3). ESI-MS: m/z 376.4 (M+1), $C_{20}H_{17}N_5O_3$ [375.13].

4.1.12. 4-(5-Amino-2-(mesityloxy)pyrimidin-4-ylamino) benzonitrile (7b)

White powder, yield: 75.5%. mp: 207–209 °C. ^{1}H NMR (400 MHz, DMSO-d_6, ppm) δ: 8.99 (s, 1H, NH), 7.72 (s, 1H, C_6-pyrimidine-H), 7.68 (d, 2H, J = 8.84 Hz, Ph′-H), 7.49 (d, 2H, J = 8.84 Hz, 2H, Ph′-H), 6.94 (s, 2H, Ph-H), 4.90 (s, 2H, NH_2), 2.30 (s, 3H, CH_3), 1.98 (s, 6H, 2 × CH_3). ^{13}C NMR (100 MHz, DMSO-d_6, ppm) δ: 156.55 (C_2-pyrimidine), 150.30 (C_4-pyrimidine), 148.93 (C_1-Ph'-N), 144.83 (C_6-pyrimidine), 142.02 (C_1-Ph-O), 133.94, 132.97 (2 × C), 130.53 (2 × C), 129.39 (2 × C), 125.03, 119.80, 119.52 (2 × C), 103.39, 20.80 (CH_3), 16.28 (2 × CH_3). ESI-MS: m/z 346.3 (M+1), 368.2 (M+23), $C_{20}H_{19}N_5O$ [345.16].

4.1.13. N-(4-(4-Cyanophenylamino)-2-(mesityloxy)pyrimidin-5-yl)-2,2,2-trifluoro-acetamide (8b)

White powder, yield: 52.2%. mp: 204–208 °C. ^{1}H NMR (400 MHz, DMSO-d_6, ppm) δ: 9.21 (s, 1H, C_6-pyrimidine-H), 8.18 (d, J = 8.40 Hz, 2H, Ph′-H), 7.94 (d, J = 8.40 Hz, 2H, Ph′-H), 6.91 (s, 2H, Ph-H), 2.24 (s, 3H, CH_3), 1.97 (s, 6H, 2 × CH_3). ^{13}C NMR (100 MHz, DMSO-d_6, ppm) δ: 162.37 (C_2-pyrimidine), 162.34 (C_4-pyrimidine), 156.09 (C_6-pyrimidine), 153.31 (C_1-Ph′-N), 148.25 (C_1-Ph-O), 136.71, 134,77, 134.23 (2 × C), 130.00 (2 × C), 129.75 (2 × C), 129.58, 128.71, 119.82, 118.37, 117.11, 113.81, 20.79 (CH_3), 16.45 (2 × CH_3). ESI-MS: m/z 424.4 ($C_{22}H_{20}F_2N_5O_2^+$), $C_{22}H_{18}F_3N_5O_2$ [441.14].

4.1.14. N-(4-(4-Cyanophenylamino)-2-(mesityloxy)pyrimidin-5-yl) acetamide (9b)

White powder, yield: 49.9%. mp: 222–226 °C. ^{1}H NMR (400 MHz, DMSO-d_6, ppm) δ: 8.62 (s, 1H, NH), 8.35 (s, 1H, C_6-pyrimidine-H), 8.20 (s, 1H, NH), 7.39 (dd, J_1 = 32.00 Hz, J_2 = 8.40 Hz, 4H, Ph′-H), 6.93 (s, 2H, Ph-H), 2.35 (s, 3H, CH_3), 2.30 (s, 3H, CH_3), 2.07 (s, 6H, 2 × CH_3). ^{13}C NMR (100 MHz, DMSO-d_6, ppm) δ: 171.13 (C=O), 161.89 (C_2-pyrimidine), 155.60 (C_4-pyrimidine), 153.41 (C_1-Ph-O), 148.04 (C_6-pyrimidine), 142.74 (C_1-Ph′-N), 135.09, 132.78 (2 × C), 130.23 (2 × C), 129.32 (2 × C), 119.92 (2 × C), 119.23, 113.76, 105.50, 42.26 (CH_3), 23.61, 16.37 (2 × CH_3). ESI-MS: m/z 388.4 (M+1), $C_{20}H_{15}N_5O_4$ [387.17].

4.1.15. 4-(5-Nitro-2-(2,4,6-trichlorophenoxy)pyrimidin-4-ylamino) benzonitrile (6c)

Yellow crystals, yield: 66.9%. mp: 150–153 °C. ^{1}H NMR (400 MHz, DMSO-d_6, ppm) δ: 10.54 (s, 1H, NH), 9.29 (s, 1H, C_6-pyrimidine-H), 7.89 (s, 2H, Ph-H), 7.70 (d, J = 8.68 Hz, 2H, Ph′-H), 7.53 (d, J = 8.68 Hz, 2H, Ph′-H). ^{13}C NMR (100 MHz, DMSO-d_6, ppm) δ: 163.35 (C_2-pyrimidine), 160.51 (C_4-pyrimidine), 154.76 (C_6-pyrimidine), 144.39 (C_1-Ph′-N), 141.09 (C_1-Ph-O), 132.87 (2 × C), 132.00, 129.49 (2 × C), 129.31 (2 × C), 126.87, 126.65 (2 × C), 118.99, 108.01.

ESI-MS: *m/z* 436.3 (M+1), 438.3 (M+3), 440.4 (M+5), $C_{17}H_8Cl_3N_5O_3$ [434.97].

4.1.16. 4-(5-Amino-2-(2,4,6-trichlorophenoxy)pyrimidin-4-ylamino)benzonitrile (7c)

White powder, yield: 56.9%. mp: 150–153 °C. ^{1}H NMR (400 MHz, DMSO-d_6, ppm) δ: 9.01 (s, 1H, NH), 7.87 (s, 2H, Ph-H), 7.74 (s, 1H, C_6-pyrimidine-H), 7.65 (m, 4H, Ph′-H), 5.00 (s, 2H, NH). ^{13}C NMR (100 MHz, DMSO-d_6, ppm) δ: 154.92 (C_2-pyrimidine), 150.21 (C_4-pyrimidine), 145.78 (C_6-pyrimidine), 144.34 (C_1-Ph′-N), 141.33 (C_1-Ph-O), 133.10 (2 × C), 130.68, 130.26 (2 × C), 129.29 (2 × C), 126.32, 119.81 (2 × C), 119.65, 104.05. ESI-MS: *m/z* 406.4 (M+1), 408.4 (M+3), 410.4 (M+5), $C_{17}H_{10}Cl_3N_5O$ [405.00].

4.1.17. N-(4-(4-Cyanophenylamino)-2-(2,4,6-trichlorophenoxy) pyrimidin-5-yl)-2,2,2-trifluoroacetamide (8c)

Brown oily solid, yield: 41.2%. ^{1}H NMR (400 MHz, DMSO-d_6, ppm) δ: 9.31 (s, 1H, C_6-pyrimidine-H), 8.20 (d, J = 8.48 Hz, 2H, Ph′-H), 7.98 (d, J = 8.48 Hz, 2H, Ph′-H) 7.87 (s, 2H, Ph-H). ^{13}C NMR (100 MHz, DMSO-d_6, ppm) δ: 160.73 (C_2-pyrimidine), 156.07 (C_4-pyrimidine), 153.28(C_6-pyrimidine), 144.89 (C_1-Ph′-N), 142.85 (C_1-Ph-O), 136.51, 134.26 (2 × C), 131.53, 129.74 (2 × C), 129.64 (2 × C), 129.46 (2 × C), 118.32, 116.99, 114.28, 113.97. ESI-MS: *m/z* 484.2 ($C_{19}H_{11}Cl_3F_2N_5O_2^+$), 586.2 ($C_{19}H_{11}Cl_3F_2N_5O_2^+$ +2), $C_{19}H_9Cl_3F_3N_5O_2$ [500.98].

4.1.18. N-(4-(4-Cyanophenylamino)-2-(2,4,6-trichlorophenoxy) pyrimidin-5-yl) acetamide (9c)

White powder, yield: 40.5%. ^{1}H NMR (400 MHz, DMSO-d_6, ppm) δ: 9.40 (s, 1H, NH), 9.29 (s, 1H, NH), 8.20 (s, 1H, C_6-pyrimidine-H), 7.90 (s, 2H, Ph-H) 7.63 (m, 4H, Ph′-H), 2.09 (s, 3H, CH_3). ^{13}C NMR (100 MHz, DMSO-d_6, ppm) δ: 170.29 (C═O), 160.01 (C_2-pyrimidine), 156.83 (C_4-pyrimidine), 155.90 (C_1-Ph-O), 145.20 (C_6-pyrimidine), 143.36 (C_1-Ph′-N), 133.04 (2 × C), 131.26, 129.92 (2 × C), 128.99 (2 × C), 121.03 (2 × C), 119.44, 115.66, 105.16, 23.84 (CH_3). ESI-MS: *m/z* 448.2 (M+1), 450.2 (M+3), 452.2 (M+5), $C_{19}H_{12}Cl_3N_5O_2$ [447.01].

4.1.19. 4-(5-Nitro-2-(2,4,6-tribromophenoxy)pyrimidin-4-ylamino) benzonitrile (6d)

Yellow crystals, yield: 66.4%. mp: 183–187 °C. ^{1}H NMR (400 MHz, DMSO-d_6, ppm) δ: 10.52 (s, 1H, NH), 9.31 (s, 1H, C_6-pyrimidine-H), 8.12 (s, 2H, Ph-H), 7.67 (d, J = 8.60 Hz, 2H, Ph′-H), 7.15 (d, J = 8.40 Hz, 2H, Ph′-H). ^{13}C NMR (100 MHz, DMSO-d_6, ppm) δ: 163.32 (C_2-pyrimidine), 160.54 (C_4-pyrimidine), 154.56 (C_6-pyrimidine), 147.03 (C_1-Ph′-N), 141.08 (C_1-Ph-O), 135.43 (2 × C), 132.87 (2 × C), 126.67, 124.42 (2 × C), 120.32, 118.99, 118.79 (2 × C), 107.94. ESI-MS: *m/z* 568.1 (M+1), 570.1 (M+3), 572.1 (M+5), $C_{17}H_8Br_3N_5O_3$ [566.82].

4.1.20. 4-(5-Amino-2-(2,4,6-tribromophenoxy)pyrimidin-4-ylamino)benzonitrile (7d)

White powder, yield: 55.8%. mp: 160–164 °C. ^{1}H NMR (400 MHz, DMSO-d_6, ppm) δ: 8.98 (s, 1H, NH), 8.09 (s, 2H, Ph-H), 7.74 (s, 1H, C_6-pyrimidine-H), 7.63 (dd, J_1 = 18.24 Hz, J_2 = 8.96 Hz, 4H, Ph′-H), 4.97 (s, 2H, NH). ^{13}C NMR (100 MHz, DMSO-d_6, ppm) δ: 154.84 (C_2-pyrimidine), 150.08 (C_4-pyrimidine), 148.30 (C_6-pyrimidine), 144.38 (C_1-Ph′-N), 141.41 (C_1-Ph-O), 135.23 (2 × C), 133.09 (2 × C), 126.18, 119.95 (2 × C), 119.75 (2 × C), 119.68, 118.93, 103.94. ESI-MS: *m/z* 538.1 (M+1), 540.1 (M+3), 542.0 (M+5), 544.1 (M+7), $C_{17}H_{10}Br_3N_5O$ [536.84].

4.1.21. N-(4-(4-Cyanophenylamino)-2-(2,4,6-tribromophenoxy) pyrimidin-5-yl)-2,2,2-trifluoroacetamide (8d)

Brown oily solid, yield: 40.7%. ^{1}H NMR (400 MHz, DMSO-d_6, ppm) δ: 10.42 (s, 1H, NH), 9.21 (s, 1H, C_6-pyrimidine-H), 8.38 (s, 2H, Ph-H), 7.97 (d, J = 8.60 Hz, 2H, Ph′-H), 7.05 (d, J = 8.40 Hz, 2H, Ph′-H). ^{13}C NMR (100 MHz, DMSO-d_6, ppm) δ: 164.32 (C_2-pyrimidine), 163.44 (C_4-pyrimidine), 158.55 (C_6-pyrimidine), 150.66, 148.13 (C_1-Ph′-N), 146.08 (C_1-Ph-O), 136.45 (2 × C), 132.89 (2 × C), 127.77, 125.32 (2 × C), 122.42, 119.97, 118.71 (2 × C), 110.21, 107.95. ESI-MS: *m/z* 538.0 ($C_{17}H_{11}Br_3N_5O^+$), 540.0 ($C_{17}H_{10}Br_3N_5O^+$ +2), 633.8 (M+1), 636.0 (M+3), 637.8 (M+5), $C_{19}H_9Br_3F_3N_5O_2$ [632.83].

4.1.22. N-(4-(4-Cyanophenylamino)-2-(2,4,6-tribromophenoxy) pyrimidin-5-yl)aceta-mide (9d)

White powder, yield: 45.6%. mp: 178–180 °C. ^{1}H NMR (400 MHz, DMSO-d_6, ppm) δ: 9.39 (s, 1H, NH), 9.27 (s, 1H, NH), 8.20 (s, 1H, C_6-pyrimidine-H), 8.12 (s, 2H, Ph-H), 7.61 (s, 4H, Ph′-H), 2.09 (s, 3H, CH_3). ^{13}C NMR (100 MHz, DMSO-d_6, ppm) δ: 170.26 (C═O), 159.93 (C_2-pyrimidine), 156.68 (C_4-pyrimidine), 155.96 (C_1-Ph-O), 147.78 (C_6-pyrimidine), 143.41 (C_1-Ph′-N), 135.33 (2 × C), 133.02 (2 × C), 120.93 (2 × C), 119.54 (2 × C), 119.50, 119.45, 115.10, 105.06, 23.85 (CH_3). ESI-MS: *m/z* 579.9 (M+1), 582.0 (M+3), 583.9 (M+5), 586.0 (M+7), $C_{19}H_{12}Br_3N_5O_2$ [578.85].

4.1.23. 4-(2-(4-Bromo-2,6-dimethylphenoxy)-5-nitropyrimidin-4-ylamino)benzonitrile (6e)

Yellow crystals, yield: 70.0%. mp: 190–195 °C. ^{1}H NMR (400 MHz, DMSO-d_6, ppm) δ: 10.44 (s, 1H, NH), 9.35 (s, 1H, C_6-pyrimidine-H), 7.49 (d, J = 8.68 Hz, 2H, Ph-H), 7.39 (d, J = 8.68 Hz, 2H, Ph′-H), 7.26 (s, 2H, Ph′-H), 2.12 (s, 6H, 2 × CH_3). ^{13}C NMR (100 MHz, DMSO-d_6, ppm) δ: 165.25 (C_2-pyrimidine), 160.44 (C_4-pyrimidine), 154.37 (C_6-pyrimidine), 149.17 (C_1-Ph′-N), 140.27 (C_1-Ph-O), 133.12 (2 × C), 132.99, 132.50, 131.75 (2 × C), 124.67, 121.43 (2 × C), 119.16, 118.29, 108.71, 16.17 (2 × CH_3). ESI-MS: *m/z* 440.4 (M+1), 442.4 (M+3), $C_{19}H_{14}BrN_5O_3$ [439.03].

4.1.24. 4-(5-Amino-2-(4-bromo-2,6-dimethylphenoxy)pyrimidin-4-ylamino)benzonitrile (7e)

White powder, yield: 55.8%. mp: 160–164 °C. ^{1}H NMR (400 MHz, DMSO-d_6, ppm) δ: 8.88 (s, 1H, NH), 7.73 (s, 1H, C_6-pyrimidine-H), 7.64 (d, J = 8.88 Hz, 2H, Ph′-H), 7.53 (d, J = 8.88 Hz, 2H, Ph′-H), 7.26 (s, 2H, Ph-H), 4.87 (s, 2H, NH_2), 2.02 (s, 6H, CH_3). ^{13}C NMR (100 MHz, DMSO-d_6, ppm) δ: 156.09 (C_2-pyrimidine), 150.32 (C_4-pyrimidine), 150.03 (C_6-pyrimidine), 144.65 (C_1-Ph′-N), 141.92 (C_1-Ph-O), 133.49 (2 × C), 130.30 (2 × C), 128.91, 128.29 (2 × C), 125.31, 119.73, 119.57 (2 × C), 103.62, 16.83 (2 × CH_3). 410.4 (M+1), 412.4 (M+3), $C_{19}H_{16}BrN_5O$ [409.05].

4.1.25. N-(2-(4-Bromo-2,6-dimethylphenoxy)-4-(4-cyanophenylamino)pyrimidin-5- yl)-2,2,2-trifluoroacetamide (8e)

Brown oily solid, yield: 50.6%. ^{1}H NMR (400 MHz, DMSO-d_6, ppm) δ: 10.34 (s, 1H, NH), 10.11 (s, 1H, NH), 9.25 (s, 1H, C_6-pyrimidine-H), 7.60 (d, J = 8.68 Hz, 2H, Ph-H), 7.48 (d, J = 8.68 Hz, 2H, Ph′-H), 7.34 (s, 2H, Ph-H), 2.32 (s, 6H, 2 × CH_3). ^{13}C NMR (100 MHz, DMSO-d_6, ppm) δ: 166.26 (C_2-pyrimidine), 161.14 (C_4-pyrimidine), 155.35 (C_6-pyrimidine), 150.67, 148.27 (C_1-Ph′-N), 147.28 (C_1-Ph-O), 133.32 (2 × C), 132.09, 132.51, 130.85 (2 × C), 125.66, 124.47 (2 × C), 119.36, 118.00, 110.22, 109.71, 16.74 (2 × CH_3). ESI-MS: *m/z* 588.3 ($C_{21}H_{17}BrF_2N_5O_2^+$), 590.3 ($C_{21}H_{17}BrF_2N_5O_2^+$ +2), $C_{21}H_{15}BrF_3N_5O_2$ [505.04].

4.1.26. N-(2-(4-Bromo-2,6-dimethylphenoxy)-4-(4-cyanophenylamino)pyrimidin-5-yl)acetamide (9e)

White powder, yield: 59.7%. mp: 145–148 °C. ^{1}H NMR (400 MHz, DMSO-d_6, ppm) δ: 9.36 (s, 1H, NH), 9.14 (s, 1H, NH), 8.16 (s, 1H, C_6-pyrimidine-H), 7.63 (dd, J_1 = 24.92 Hz, J_2 = 8.92 Hz, 4H, Ph′-H), 7.29 (s, 2H, Ph-H), 2.09 (s, 3H, CH_3), 2.05 (s, 6H, 2 × CH_3). ^{13}C NMR (100 MHz, DMSO-d_6, ppm) δ: 170.29 (C═O), 161.06 (C_2-pyrimidine), 156.73 (C_4-pyrimidine), 156.02 (C_1-Ph-O), 149.50 (C_6-

pyrimidine), 143.74 (C_1-Ph′-N), 133.17 (2 × C), 132.96 (2 × C), 129.42, 128.56 (2 × C), 120.59 (2 × C), 119.55, 114.72, 104.62, 23.85 (CH_3), 16.33 (2 × CH_3). ESI-MS: *m/z* 452.3 (M+1), 454.3 (M+3), $C_{21}H_{18}BrN_5O_2$ [451.06].

4.1.27. 4-(2-(2,6-Dichlorophenoxy)-5-nitropyrimidin-4-ylamino) benzonitrile (6f)

Yellow powder, yield: 62.2%. mp: 193–196 °C. ^{1}H NMR (400 MHz, DMSO-d_6, ppm) *δ*: 10.45 (s, 1H, NH), 9.30 (s, 1H, C_6-pyrimidine-H), 7.60 (s, 4H, Ph′-H), 7.32 (t, *J* = 8.48 Hz, 1H, C_4-Ph-H), 6.85 (d, *J* = 8.52 Hz, 2H, Ph-H). ^{13}C NMR (100 MHz, DMSO-d_6, ppm) *δ*: 164.54 (C_2-pyrimidine), 160.76 (C_4-pyrimidine), 154.59 (C_6-pyrimidine), 139.95 (C_1-Ph′-N), 133.17 (4 × C), 133.00, 125.67, 122.69 (4 × C), 121.84, 118.29, 109.25. ESI-MS: *m/z* 402.4 (M+1), 404.4 (M+3), $C_{17}H_9Cl_2N_5O_3$ [401.01].

4.1.28. 4-(5-Amino-2-(2,6-dichlorophenoxy)pyrimidin-4-ylamino) benzonitrile (7f)

White crystals, yield: 78.2%. mp: 114–117 °C. ^{1}H NMR (400 MHz, DMSO-d_6, ppm) *δ*: 8.95 (s, 1H, NH), 7.76 (s, 1H, C_6-pyrimidine-H), 7.64 (m, 6H, Ph-H, Ph′-H), 7.41 (t, 1H, *J* = 8.80 Hz, C_4-Ph-H), 4.96 (s, 2H, NH_2). ^{13}C NMR (100 MHz, DMSO-d_6, ppm) *δ*: 155.11 (C_2-pyrimidine), 150.04 (C_4-pyrimidine), 146.36 (C_1-Ph′-N), 144.51 (C_6-pyrimidine), 141.34 (C_1-Ph-O), 133.08 (2 × C), 129.64 (2 × C), 129.33 (2 × C), 127.68, 126.21, 119.73, 119.56 (2 × C), 103.75. ESI-MS: *m/z* 372.2 (M+1), 374.2 (M+3), 376.3 (M+5), 378.3 (M+7), $C_{17}H_{11}Cl_2N_5O$ [371.03].

4.1.29. N-(4-(4-Cyanophenylamino)-2-(2,6-dichlorophenoxy) pyrimidin-5-yl)-2,2,2-trifluoroacetamide (8f)

Brown oily solid, yield: 58.3%. mp: 205–208 °C. ^{1}H NMR (400 MHz, DMSO-d_6, ppm) *δ*: 9.09 (s, 1H, C_6-pyrimidine-H), 7.91 (d, *J* = 8.60 Hz, 2H, Ph′-H), 7.64 (d, *J* = 8.60 Hz, 2H, Ph′-H), 7.41 (d, *J* = 8.08 Hz, 2H, Ph-H), 7.21 (t, *J* = 8.08 Hz, 1H, C_4-Ph-H). ^{13}C NMR (100 MHz, DMSO-d_6, ppm) *δ*: 161.51 (C_2-pyrimidine), 155.05 (C_4-pyrimidine), 153.45 (C_6-pyrimidine), 145.59 (C_1-Ph-O), 142.24 (C_1-Ph′-N), 135.72, 133.70 (2 × C), 129.16 (2 × C), 128.52 (2 × C), 127.09 (2 × C), 128.31 (2 × CN), 119.26, 117.36, 114.61. ESI-MS: *m/z* 450.2 ($C_{19}H_{12}Cl_2F_2N_5O_2^+$ +1), 452.2 ($C_{19}H_{12}Cl_2F_2N_5O_2^+$ +2), $C_{19}H_{10}Cl_2F_3N_5O_2$ [467.02].

4.1.30. N-(4-(4-Cyanophenylamino)-2-(2,6-dichlorophenoxy) pyrimidin-5-yl)acetamide (9f)

White crystals, yield: 60.7%. mp: 158–161 °C. ^{1}H NMR (400 MHz, DMSO-d_6, ppm) *δ*: 9.38 (s, 1H, NH), 9.22 (s, 1H, NH), 8.20 (s, 1H, C_6-pyrimidine-H), 7.67 (d, *J* = 8.0 Hz, 2H, Ph-H), 7.59 (s, 4H, Ph′-H), 7.44 (t, *J* = 8.40 Hz, 1H, C_4-Ph-H), 2.09 (s, 3H, CH_3) ^{13}C NMR (100 MHz, DMSO-d_6, ppm) *δ*: 170.33 (C═O), 160.28 (C_2-pyrimidine), 156.79 (C_4-pyrimidine), 156.06 (C_1-Ph-O), 145.77 (C_6-pyrimidine), 143.45 (C_1-Ph′-N), 133.09 (2 × C), 129.76 (2 × C), 128.98 (2 × C), 128.23, 120.66 (2 × C), 119.49, 115.43, 104.93, 23.86 (CH_3). ESI-MS: *m/z* 414.3 (M+1), 416.3 (M+3), $C_{19}H_{13}Cl_2N_5O_2$ [413.04].

4.1.31. 4-(2-(4-Formyl-2,6-dimethylphenoxy)-5-nitropyrimidin-4-ylamino)benzonitrile (6g)

Yellow crystals, yield: 66.9%. mp: 171–173 °C. ^{1}H NMR (400 MHz, DMSO-d_6, ppm) *δ*: 10.46 (s, 1H, NH), 10.01 (s, 1H, CHO), 9.29 (s, 1H, C_6-pyrimidine-H), 7.76 (s, 2H, Ph-H), 7.64 (s, 4H, Ph′-H), 2.15 (s, 6H, 2 × CH_3). ^{13}C NMR (100 MHz, DMSO-d_6, ppm) *δ*: 192.68 (H–C═O), 164.27 (C_2-pyrimidine), 160.45 (C_4-pyrimidine), 154.84 (C_1-Ph-O), 154.54 (C_6-pyrimidine), 141.39 (C_1-Ph′-N), 134.44, 132.58 (2 × C), 131.81 (2 × C), 130.56 (2 × C), 126.28, 125.12, 123.65 (2 × C), 119.02, 16.31 (2 × CH_3). ESI-MS: *m/z* 390.3 (M+1), 407.5 (M+17), $C_{20}H_{15}N_5O_4$ [389.11].

4.1.32. 4-(5-Amino-2-(4-formyl-2,6-dimethylphenoxy)pyrimidin-4-ylamino)benzonitrile (7g)

White powder, yield: 78.2%. mp: 293–297 °C. ^{1}H NMR (400 MHz, DMSO-d_6, ppm) *δ*: 10.02 (s, 1H, CHO), 9.17 (s, 1H, NH), 7.79 (m, 3H, C_6-pyrimidine-H, Ph′-H), 7.68 (d, 2H, *J* = 8.80 Hz, Ph-H), 7.48 (d, 2H, *J* = 8.80 Hz, Ph-H), 5.07 (s, 2H, NH_2). ^{13}C NMR (100 MHz, DMSO-d_6, ppm) *δ*: 192.81 (CHO), 156.10 (C_2-pyrimidine), 155.76 (C_4-pyrimidine), 150.26 (C_1-Ph′-N), 144.68 (C_6-pyrimidine), 141.47 (C_1-Ph-O), 133.59, 133.00 (2 × C), 132.48 (2 × C), 132.29, 130.45 (2 × C) 125.75, 126.21, 119.73, 119.75 (2 × C), 103.56. ESI-MS: *m/z* 360.4 (M+1), 382.5 (M+23), $C_{20}H_{17}N_5O_2$ [359.14].

4.1.33. N-(4-(4-Cyanophenylamino)-2-(4-formyl-2,6-dimethylphenoxy)pyrimidin-5-yl)- 2,2,2-trifluoroacetamide (8g)

White powder, yield: 54.4%. mp: 179–182 °C. ^{1}H NMR (400 MHz, DMSO-d_6, ppm) *δ*: 9.94 (s, 1H, H–C═O), 9.13 (s, 1H, C_6-pyrimidine-H), 8.47 (b, 1H, NH) 7.93 (d, *J* = 8.44 Hz, 2H, Ph′-H), 7.67 (s, 2H, Ph-H), 2.18 (s, 6H, 2 × CH_3). ^{13}C NMR (100 MHz, DMSO-d_6, ppm) *δ*: 192.27 (CHO), 161.82 (C_2-pyrimidine), 154.07 (C_4-pyrimidine), 153.47 (C_6-pyrimidine), 135.47 (C_1-Ph-O), 133.86 (2 × C), 133.83 (4 × C), 131.89 (2 × C), 130.74 (2 × C), 128.40, 128.26 (2 × C), 117.16, 114.61, 16.51 (2 × CH_3). ESI-MS: *m/z* 438.4 ($C_{22}H_{18}F_2N_5O_3^+$), $C_{22}H_{16}F_3N_5O_3$ [455.12].

4.1.34. N-(4-(4-Cyanophenylamino)-2-(4-formyl-2,6-dimethylphenoxy)pyrimidin-5-yl) acetamide (9g)

White crystals, yield: 53.3%. mp: 167–170 °C. ^{1}H NMR (400 MHz, DMSO-d_6, ppm) *δ*: 10.00 (s, 1H, NH), 9.94 (s, 1H, NH), 9.81 (s, 1H, CHO), 9.23 (s, 1H, C_6-pyrimidine-H), 7.45 (s, 2H, Ph-H), 7.64 (s, 4H, Ph′-H), 2.15 (s, 6H, 2 × CH_3), 2.00 (s, 3H, CH_3). ^{13}C NMR (100 MHz, DMSO-d_6, ppm) *δ*: 193.88 (H–C═O), 166.37 (C_2-pyrimidine), 161.44 (C_4-pyrimidine), 160.34 (C_1-Ph-O), 155.20 (C_6-pyrimidine), 144.29 (C_1-Ph′-N), 135.46, 133.58 (2 × C), 132.51 (2 × C), 131.66 (2 × C), 127.28, 125.14, 122.25 (2 × C), 120.22, 20.35 (CH_3), 16.31 (2 × CH_3). ESI-MS: *m/z* 402.3 (M+1), 424.4 (M+23), $C_{22}H_{19}N_5O_3$ [401.15].

4.2. Biological activity evaluation

4.2.1. In vitro anti-HIV assay

Evaluation of the antiviral activity of the compounds against HIV-1 strain IIIB and HIV-2 strain (ROD) in MT-4 cells was performed using the MTT assay as previously described [23]. Stock solutions (10 × final concentration) of test compounds were added in 25-μL volumes to two series of triplicate wells so as to allow simul-taneous evaluation of their effects on mock- and HIV-infected cells at the beginning of each experiment. Serial fivefold dilutions of test compounds were made directly in flat-bottomed 96-well microti-ter trays using a Biomek 3000 robot (Beckman instruments, Fuller-ton, CA). Untreated control HIV- and mock-infected cell samples were included for each sample.

HIV-1 (IIIB) [24] or HIV-2 (ROD) [25] stock (50 μL) at 100–300 CCID50 (cell culture infectious dose) or culture medium was added to either the infected or mock-infected wells of the microtiter tray. Mock-infected cells were used to evaluate the effect of test compound on uninfected cells in order to assess the cytotoxicity of the test compound. Exponentially growing MT-4 cells were centrifuged for 5 min at 1000 rpm and the supernatant was discarded. The MT-4 cells were resuspended at 6 × 10^5 cells/mL, and 50-μL volumes were transferred to the microtiter tray wells. Five days after infection, the viability of mock- and HIV-infected cells was examined spectrophotometrically by the MTT assay.

The MTT assay is based on the reduction of yellow colored 3-(4,5-dimethylthiazol-2-yl)-2,5-diphenyltetrazolium bromide (MTT) (Acros Organics, Geel, Belgium) by mitochondrial dehydro-genase of metabolically active cells to a blue-purple

formazan that can be measured spectrophotometrically. The absorbances were read in an eight-channel computer-controlled photometer (Multi-scan Ascent Reader, Labsystems, Helsinki, Finland), at two wave-lengths (540 and 690 nm). All data were calculated using the median OD (optical density) value of tree wells. The 50% cytotoxic concentration (CC_{50}) was defined as the concentration of the test compound that reduced the absorbance (OD540) of the mock-in-fected control sample by 50%. The concentration achieving 50% protection from the cytopathic effect of the virus in infected cells was defined as the 50% effective concentration (EC_{50}).

4.2.2. HIV-1 RT inhibition assay

A RT assay kit produced by Roche was used for the RT inhibition assay. All the reagents for performing the RT reaction are contained in the kit and the ELSIA procedures for RT inhibition assay was performed as described in the kit protocol [26–28].

Briefly, the reaction mixture containing HIV-1 reverse transcriptase (RT) enzyme, reconstituted template and viral nucleotides (digoxigenin (DIG)-dUTP, biotin-dUTP and dTTP) in the incubation buffer with or without inhibitors was incubated for 1 h at 37 °C. Then, the reaction mixture was transferred to a streptavidine-coated microtiter plate (MTP) and incubated for another 1 h at 37 °C. The biotin-labeled dNTPs that was incorporated in cDNA chain in the presence of RT were bound to streptavidine. The unbound dNTPs were removed by rinsing using washing buffer followed by the addition of anti-DIG-POD working solution into the MTPs. After incubation for 1 h at 37 °C, the DIG-labeled dNTPs incorporated in cDNA were bound to the anti-DIG-POD antibody. The unbound anti-DIG-PODs were removed and the peroxide substrate (ABST) solution was added to the MTPs. Incubation of the reaction mixture at 25 °C until a green color was sufficiently developed for detection. The absorbance of the sample was determined at O.D. 405 nm using microtiter plate ELISA reader. The percentage inhibitory activity of RT inhibitors was calculated by formula as given below:

%Inhibition = [O.D. value with RT but without inhibitors − O.D. va lue with RT and inhibitors]/[O.D. value with RT and inhibitors − O.D. value without RT and inhibitors]

The IC_{50} values corresponded to the concentrations of the inhibitors required to inhibit biotin-dUTP incorporation by 50%.

4.3. Molecular simulation

The molecules **7a** for docking was optimized for 2000-generations until the maximum derivative of energy became 0.005 kcal/(mol*Å), using the Tripos force field. Charges were computed and added according to Gasteiger–Huckel parameters. The published three-dimensional crystal structures of RT complexes with TMC125 (PDB code: 3MEC) and TMC278 (PDB code: 3BGR) were retrieved from the Protein Data Bank and were used for the docking studies by means of surflex-docking module of Sybyl-X 1.1 [29]. The protein was prepared by using the Biopolymer application accompanying Sybyl: The bound ligand was extracted from the complexes, water molecules were removed, hydrogen atoms were added, side chain amides and side chains bumps were fixed, and charges and atom types were assigned according to AMBER99. After the protomol was generated, the optimized compounds **7a** was surflex-docked into the binding pocket of NNRTIs, with the relevant parameters set as defaults. Top-scoring poses were shown by the software of PyMOL version 1.5 (http://www.pymol.org/), in overlap with the bound ligand (TMC-125/TMC-278) in the binding site of RT. The secondary structure of RT is shown in cartoons, and only the key residues for interactions with the inhibitors were shown in sticks and labeled. The potential hydrogen-bondings were presented by dashed lines.

Notes

The authors declare no competing financial interest.

Acknowledgments

We thank K. Erven, K. Uyttersprot and C. Heens for technical assistance with the HIV assays. The financial support from the National Natural Science Foundation of China (NSFC No. 81273354, No. 81102320, No. 30873133, No. 30772629, No. 30371686), Key Project of NSFC for International Cooperation (No. 30910103908), Research Fund for the Doctoral Program of Higher Education of China (Nos. 20110131130005, 20110131120037), Natural Science Foundation of Shandong Province (ZR2009CM016) and KU Leuven (GOA 10/014).

Appendix A. Supplementary data

Supplementary data related to this article can be found at http://dx.doi.org/10.1016/j.ejmech.2014.04.036.

References

[1] UNAIDS, Global AIDS Report, 2012.
[2] B. Ledergerber, M. Egger, M. Opravil, A. Telenti, B. Hirschel, M. Battegay, P. Vernazza, P. Sudre, M. Flepp, H. Furrer, P. Francioli, R. Weber, Lancet 353 (1999) 863–868.
[3] G.M. Lucas, R.E. Chaisson, R.D. Moore, Annals of Internal Medicine 131 (1999) 81–87.
[4] B. Hirschel, P. Francioli, The New England Journal of Medicine 338 (1998) 906–908.
[5] M.P. de Béthune, Antiviral Research 85 (2010) 75–90.
[6] E. De Clercq, Journal of Medicinal Chemistry 48 (2005) 1–17.
[7] R. Pauwels, Current Opinion in Pharmacology 4 (2004) 437–446.
[8] J. Balzarini, Current Topics in Medicinal Chemistry 4 (2004) 921–944.
[9] E. De Clercq, Chem. Biodiversity 1 (2004) 44–64.
[10] http://www.fda.gov/Drugs/default.htm.
[11] P. Zhan, X. Liu, Expert Opinion on Therapeutic Patents 21 (2011) 717–796.
[12] X. Chen, P. Zhan, D. Li, E. De Clercq, X. Liu, Current Medicinal Chemistry 18 (2011) 359–376.
[13] D. Li, P. Zhan, H. Liu, C. Pannecouque, J. Balzarini, E. De Clercq, X. Liu, Bioorganic & Medicinal Chemistry 21 (2013) 2128–2134.
[14] B. Qin, X. Jiang, H. Lu, X. Tian, F. Barbault, L. Huang, K. Qian, C.H. Chen, R. Huang, S. Jiang, K.H. Lee, L. Xie, Journal of Medicinal Chemistry 53 (2010) 4906–4916.
[15] E.B. Lansdon, K.M. Brendza, M. Hung, R. Wang, S. Mukund, D. Jin, G. Birkus, N. Kutty, X.H. Liu, Journal of Medicinal Chemistry 53 (2010) 4295–4299.
[16] J. Rebehmed, F. Barbault, C. Teixeira, F. Maurel, Journal of Computer-Aided Molecular Design 22 (2008) 831–841.
[17] Y. Shao, A.G. Cole, M.R. Brescia, L.Y. Qin, J. Duo, T.M. Stauffer, L.L. Rokosz, B.F. McGuinness, I. Henderson, Bioorganic & Medicinal Chemistry Letters 19 (2009) 1399–1402.
[18] J. Yang, L.J. Wang, J.J. Liu, L. Zhong, R.L. Zheng, Y. Xu, P. Ji, C.H. Zhang, W.J. Wang, X.D. Lin, L.L. Li, Y.Q. Wei, S.Y. Yang, Journal of Medicinal Chemistry 55 (2012) 10685–10699.
[19] X. Tian, B. Qin, Z. Wu, X. Wang, H. Lu, S.L. Morris-Natschke, C.H. Chen, S. Jiang, K.H. Lee, L. Xie, Journal of Medicinal Chemistry 53 (2010) 8287–8297.
[20] X.Q. Feng, Y.H. Liang, Z.S. Zeng, F.E. Chen, J. Balzarini, C. Pannecouque, E. De Clercq, ChemMedChem 4 (2009) 219–224.
[21] V. Stockmann, J.M. Bakke, P. Bruheim, A. Fiksdahl, Tetrahedron 65 (2009) 3668–3672.
[22] S. Darvesh, R.S. McDonald, K.V. Darvesh, D. Mataija, S. Mothana, H. Cook, K.M. Carneiro, N. Richard, R. Walsh, E. Martin, Bioorganic & Medicinal Chemistry 14 (2006) 4586–4599.
[23] C. Pannecouque, D. Daelemans, E. De Clercq, Nature Protocols 3 (2008) 427–434.
[24] X. Chen, P. Zhan, C. Pannecouque, J. Balzarini, E. De Clercq, X. Liu, European Journal of Medicinal Chemistry 51 (2012) 60–66.

[25] F. Clavel, D. Guétard, F. Brun-Vézinet, S. Chamaret, M. Rey, M. Santos-Ferreira, A. Laurent, C. Dauguet, C. Katlama, C. Rouzioux, D. Klatzmann, J.L. Champalimaud, L. Montagnier, Science 233 (1986) 343–346.
[26] R.K. Rawal, R. Tripathi, S. Katti, C. Pannecouque, E. De Clercq, Bioorganic & Medicinal Chemistry 15 (2007) 1725–1731.
[27] R.K. Rawal, R. Tripathi, S. Katti, C. Pannecouque, E. De Clercq, European Journal of Medicinal Chemistry 43 (2008) 2800–2806.
[28] S. Fatima, A. Sharma, R. Saxena, R. Tripathi, S.K. Shukla, S.K. Pandey, R. Tripathi, R.P. Tripathi, European Journal of Medicinal Chemistry 55 (2012) 195–204.
[29] K. Das, J.D. Bauman, A.D. Clark Jr., Y.V. Frenkel, P.J. Lewi, A.J. Shatkin, S.H. Hughes, E. Arnold, Proceedings of the National Academy of Sciences 105 (2008) 1466–1471.